**Title**
Carbon Dioxide and Methane Emissions from a California Salt Marsh



**Author**
Wang, Jian

**Publication Date**
2017

Peer reviewed|Thesis/dissertation

UNIVERSITY OF CALIFORNIA

Santa Barbara

# Carbon Dioxide and Methane Emissions from a California Salt Marsh

A Thesis submitted in partial satisfaction of the

requirements for the degree Master of Arts

in Geography

by

Jian Wang

Committee in charge:

Professor Jennifer King, Chair

Professor Oliver Chadwick

Professor John Melack

January 2018

The thesis of Jian Wang is approved.

John Melack

Oliver Chadwick

Jennifer King, Committee Chair

December 2017

ACKNOWLEDGEMENTS

I would like to express my deepest gratitude to my advisor, Dr. Jennifer King, for her continued guidance and support, as well as her attention to detail and use of a Socratic approach in encouraging me to explore and refine my research.

I would also like to extend my appreciation to my committee members: Dr. Oliver Chadwick; and Dr. John Melack for their sage advice during my research.

This research was funded through grants received from the UCSB Coastal Fund Grant (Grant # FALL15-07) and Earth Research Institute Summer Fellowship Program. The research would not have been possible without their generous support.

I want to thank all managers, graduate students, and research assistants of the King Lab, Schimel Lab, and D'Antonio Lab at UC Santa Barbara for their advice and field and laboratory support; specifically, Dr. Yang Lin, Keri Opalk, Eric Slessarev, Kenneth Marcus, Stephanie Ma, Michelle Oyewole, Kana Yamamoto, Noah Gluschankoff, Andrew Saunders, and Brendan Kapoor.

I appreciate the assistance to obtain permits and access to the study site from Dr. Andrew Brooks, Reserve Director of the Carpinteria Salt Marsh Reserve, University of California Natural Reserve System.

**Abstract**

Carbon Dioxide and Methane Emissions from a California Salt Marsh

By Jian Wang

Wetland carbon sequestration is offset by carbon dioxide ($CO_2$) and methane ($CH_4$) emissions for which the magnitudes remain coarsely constrained. To better understand the spatial and temporal variations of gaseous carbon fluxes from marsh soils in a Mediterranean climate, I collected air and soil samples over the course of 10 months at Carpinteria Salt Marsh Reserve (CSMR) located in the County of Santa Barbara, California. The CSMR consists of four zones characterized by differences in elevation, tidal regime, soil properties, and vegetation. Twelve static chambers were deployed among two lower marsh zones, a mudflat, and a marsh-upland transition zone for fortnightly flux measurements from September 2015 to May 2016. In August 2015 and June 2016, soil cores up to 50 cm deep were extracted near the chambers, segmented by depth, and analyzed for soil moisture, bulk density, particle size distribution, electrical conductivity, pH, organic/inorganic carbon, and total nitrogen content. Averaged over the 9-month study period, the marsh-upland transition zone had the highest $CO_2$ fluxes at $5.3 \pm 0.7$ g $CO_2$ $m^{-2}$ $d^{-1}$, followed closely by the lower marsh zones ($3.8 \pm 0.6$ g $CO_2$ $m^{-2}$ $d^{-1}$ and $2.8 \pm 0.7$ g $CO_2$ $m^{-2}$ $d^{-1}$), which were one order of magnitude higher than the $CO_2$ fluxes from the mudflat ($0.4 \pm 0.1$ g $CO_2$ $m^{-2}$ $d^{-1}$). The $CO_2$ fluxes varied significantly on a seasonal scale but were not consistently correlated with environmental variables measured. The $CH_4$ fluxes had no clear seasonal patterns, but overall $CH_4$ flux rates from the lower marsh zones ($2.2 \pm 1.5$ mg $CH_4$ $m^{-2}$ $d^{-1}$ and $1.9 \pm 0.2$ mg $CH_4$ $m^{-2}$ $d^{-1}$) surpassed those from the mudflat ($0.2 \pm 0.06$ mg $CH_4$ $m^{-2}$ $d^{-1}$) by an order of magnitude, and the marsh-upland transition zone was a net methane

sink (-0.07 ± 0.1 mg $CH_4$ $m^{-2}$ $d^{-1}$). The $CH_4$ fluxes correlated well with most soil properties by zone. Our results show that soil gaseous carbon fluxes from a coastal salt marsh vary by salt marsh zone.

# Table of Contents

# List of Tables

## List of Figures

## 1. Introduction

Concentrations of carbon dioxide ($CO_2$) and methane ($CH_4$) in the atmosphere have increased by 40% and 150% respectively, since 1750, and these increases are a main cause of global climate change (Ciais et al. 2014). Wetlands are both a major source and sink of these greenhouse gases, as their anoxic wet conditions provide environments conducive for storing carbon (carbon sequestration) and producing methane (methanogenesis). Representing 20–25% of current global $CH_4$ emissions (Mitsch et al. 2013), $CH_4$ emissions from wetlands (177 to 284 Tg $CH_4$ $yr^{-1}$) account for the largest global $CH_4$ flux from natural sources and its interannual variability (Ciais et al. 2014). However, the level of confidence remains low in modeling wetland $CH_4$ emissions due to constraints from available observational data sets, and many wetlands face challenges from global warming with changes in sea level, precipitation patterns, and increases in atmospheric $CO_2$ and temperature (Scavia et al. 2002). It is thus critical to study the dynamics and mechanisms of gaseous carbon fluxes in wetland ecosystems.

Past studies have focused on factors that influence $CH_4$ and $CO_2$ emissions from various types of wetlands. Among them, tidal saline wetlands, i.e., salt marshes and mangrove swamps, differ from peatlands or other freshwater wetlands in terms of soil chemistry and carbon biogeochemistry (Chmura et al. 2003). Ranging from arctic to subtropical regions, salt marshes are complex hydrological environments in which shallow groundwater has an interrelationship with tidal flows, which influence the temperature and movement of water, the dissolution and precipitation of salts, the oxidation/reduction of minerals and ions, and vegetation development (Taillefert et al. 2007). Many of these environmental factors have potential implications for the $CH_4$ and $CO_2$ fluxes from salt marshes.

Carbon dioxide emission is the primary mechanism of gaseous carbon loss from wetlands. $CO_2$ is produced by prokaryotic and eukaryotic organisms during aerobic respiration and by some fungi and many different groups of prokaryotes through anaerobic respiration and fermentation (Koh et al. 2009). Emission of $CO_2$ from the soil represents the combined effects of root respiration and mineralization of organic matter (Magenheimer et al. 1996). For salt marsh ecosystems, the flux of $CO_2$ is related to plant productivity, the quantity and quality of the soil organic matter (Chmura et al. 2011; Xu et al. 2014), temperature (Wilson et al. 2015), and water table position (Nyman and DeLaune 1991), as well as the rate of sulfate reduction (Magenheimer et al. 1996). Furthermore, certain salt marsh plant species induce higher $CO_2$ emission rates due to rhizosphere oxygenation from fibrous root structures and high root density.

It is generally recognized that high soil salinity may suppress $CH_4$ emissions from coastal salt marshes, although studies report different salinity thresholds ranging from 13 to 18 g/L (Bartlett et al. 1987; Poffenbarger et al. 2011; Wang et al. 2017). Salinity is an indicator of the concentrations of terminal electron acceptors (TEAs) in soil solutions such as sulfate (Bartlett et al. 1987; Poffenbarger et al. 2011; Bridgham et al. 2013). Sulfate reducing bacteria in sediments may outcompete or inhibit methanogens or oxidize $CH_4$ (Bartlett et al. 1987), which may lead to low $CH_4$ emissions from saline wetlands. However, when sulfate is depleted, despite a high salinity, the ratio of salinity to sulfate concentration ($Sal/SO_4$) is a more useful indicator of the sulfate pool (Bartlett et al. 1987; Giani et al. 1996; Poffenbarger et al. 2011). Potential salinity suppression of $CH_4$ emission is also associated with the tidal cycle as tidal flushing can replenish alternative TEAs in tidal wetland soils. Because of this, the effect of water table level on $CH_4$ fluxes is less established for salt marshes, unlike non-tidal wetlands (Deppe et al. 2010; Moore et al. 2011) or rice paddies (Meijide et al. 2011), as water table position is tightly linked to the tidal cycle, and consequently soil salinity, for tidal wetland ecosystems.

In addition to salinity, vegetation may affect $CH_4$ fluxes from salt marshes. Plant productivity can support $CH_4$ production through provision of organic substrates, the quality and quantity of which influence methanogenesis. Aerenchyma tissues can facilitate $CH_4$ emission by reducing the amount of $CH_4$ oxidation in the aerobic zone near the wetland surface (Bridgham et al. 2013). At the same time, rhizosphere methanotrophy could lead to decreased $CH_4$ emissions from a salt marsh (Martin and Moseman-Valtierra 2015). Some wetland plant species offer protection against phytotoxins commonly found in reduced, waterlogged soils by releasing oxygen to the rhizosphere. The oxygen either is directly utilized by methane-oxidizing bacteria or indirectly suppresses methanogenesis by reoxidizing alternative TEAs such as $Al^{3+}$, $Mn^{2+}$, and $Fe^{2+}$ (Laanbroek 2010).

An important ecological concept related to plants in salt marshes is salt marsh zonation. It is characteristic of intertidal salt marshes to be segregated into zones comprised of a few dominant plant species that form a distinctive assemblage and sustain other species (Moffett et al. 2010). The distribution of salt marsh macrophyte species may be associated with narrow ranges of soil topographic elevation (Silvestri et al. 2005) and likely reflects adaptations to different environmental conditions such as low nutrients and/or tidal stress (Emery et al. 2001). Climate may also play a part in salt marsh zonation, as evidenced by strong floristic, physiognomic, ecological, and zonal similarities among salt marshes of the

North American Pacific coast and the Iberian Peninsula in areas of Mediterranean climate (Peinado et al. 1995). The species-specific effects of plants on $CH_4$ and $CO_2$ emissions have been studied in wetlands of other types (Ström et al. 2005; Koh et al. 2009), but to our knowledge only one study has been published for a coastal salt marsh (Moseman-Valtierra et al. 2016). The study was conducted in a New England coastal marsh and did not find significant zonal patterns for $CH_4$ fluxes, which was attributed to methanogens being more prone to influence by physical variables (water level, salinity, temperature) than by plants. However, significant differences in $CO_2$ fluxes existed between two relatively similar native vegetated zones on top of the difference between vegetated zones and bare, inundated ponds.

With our current knowledge on wetland $CO_2$ and $CH_4$ fluxes and factors that influence them, there remains a paucity of research on the biogeochemistry of Pacific coast wetlands (Callaway et al. 2012), or of wetlands under a Mediterranean climate in general. In these salt marsh ecosystems, precipitation inputs are low and strongly seasonal. The lack of precipitation can produce hypersaline soils in high marsh areas, whereas winter rains eventually reduce soil salinities, leading to large annual variations in soil conditions with possible implications for salt marsh $CH_4$ and $CO_2$ fluxes. The lack of relevant research, the distinct seasonal pattern of the Mediterranean climate, and the strong similarities in salt marsh zonation patterns in Mediterranean climate regions around the world highlight the importance of studying $CO_2$ and $CH_4$ fluxes of these salt marsh ecosystems.

### *1.1. Research goal and hypotheses*

The overarching goal of this research was to investigate the spatial and temporal patterns of $CO_2$ and $CH_4$ fluxes from a salt marsh under a Mediterranean climate. Specifically, this study aims to (1) quantify and compare the $CO_2$ and $CH_4$ fluxes at the soil-vegetation-atmosphere interface associated with salt marsh zonation; (2) advance our understanding of how seasonality of a Mediterranean climate affects gaseous carbon fluxes; and (3) assess the environmental influences on $CO_2$ and $CH_4$ fluxes from a coastal salt marsh ecosystem. I hypothesized that emission rates of both $CH_4$ and $CO_2$ would be lower in winter as air and soil temperatures are lower. I also hypothesized that the $CH_4$ fluxes from a coastal salt marsh would be relatively low and that there would not be significant differences among different zones due to salinity suppression of methanogenesis in the lower marsh zones and high methanotrophy (methane oxidation) at the marsh-upland transition zone. In contrast, $CO_2$ flux would differ significantly by zone. The marsh-upland transition zone would likely have the highest $CO_2$ flux rates due to exclusion from inundation, whereas $CO_2$ flux from the mudflat would be the lowest due to lack of vegetation.

## 2. Materials and Methods

### *2.1. Study site*

The study was conducted at Carpinteria Salt Marsh Reserve (CSMR; 34.400°N, 119.535°W.), a site managed by the University of California Natural Reserve System. The CSMR is part of a 93-ha estuarine tidal wetland located 12 km east of Santa Barbara, California. It has a typical Mediterranean climate with a hot and dry summer and mild winter. The precipitation is usually clustered in winter months, and the average annual precipitation is about 38 cm. The climograph of the weather station (34.4141°N, 119.8796°W) closest to the CSMR is shown in Figure 1.

Four zones (Figure 2) were identified that reflect the long-term interactions of tidal regime, surface elevation, soil properties, and vegetative cover at different locations within the CSMR. Zone 1 is a low marsh zone closest to the tidal inlet to the marsh with the most complex network of channels and unrestricted tidal connectivity (and hereafter referred to as "the lower marsh zone 1"). Zone 2 (hereafter "the lower marsh zone 2") is a marsh zone bounded by an unpaved road on the west with restricted tidal connectivity. Zone 3 (hereafter "the mudflat") is a hypersaline mudflat with salt deposits at the surface during dry seasons and is likely the remnant of an alluvial fan of the Santa Monica Creek to the east before its channelization (L. Reynolds, personal communication, March 10, 2017). Zone 4 (hereafter "the transition zone") is a marsh-upland transition zone that is generally supratidal and has greater plant species diversity than the other zones. The four zones are progressively further from the ocean with a small increase in elevation (approximately 80 cm rise from Zone 1 to Zone 4 over 500 m) and large declines in inundation frequency. For instance, the lower marsh zones 1 and 2 are tidally flushed daily, and the mudflat is only inundated in winter, albeit only 30 cm higher in elevation, whereas the water table only comes close to the surface during perigean spring tides at the transition zone. Soils developed in the estuary and tidal flats are usually poorly drained, fine sandy loams (Ferren 1985). The predominant vegetation/habitat form is estuarine emergent wetland dominated by Pickleweed (*Sarcocornia pacifica*). Similar to other salt marsh ecosystems, plants found in the lower marsh zones have to cope with submergence during high tide, which restricts sediment aeration and prevents gas exchange, and with exposure during low tide, which leads to desiccation (Masselink et al. 2011, p. 184). Detailed descriptions of the biological, physical, and hydrological features of the marsh can be found in Ferren (1985), Callaway et al. (1990), Page et al. (1995), and Sadro et al. (2007).

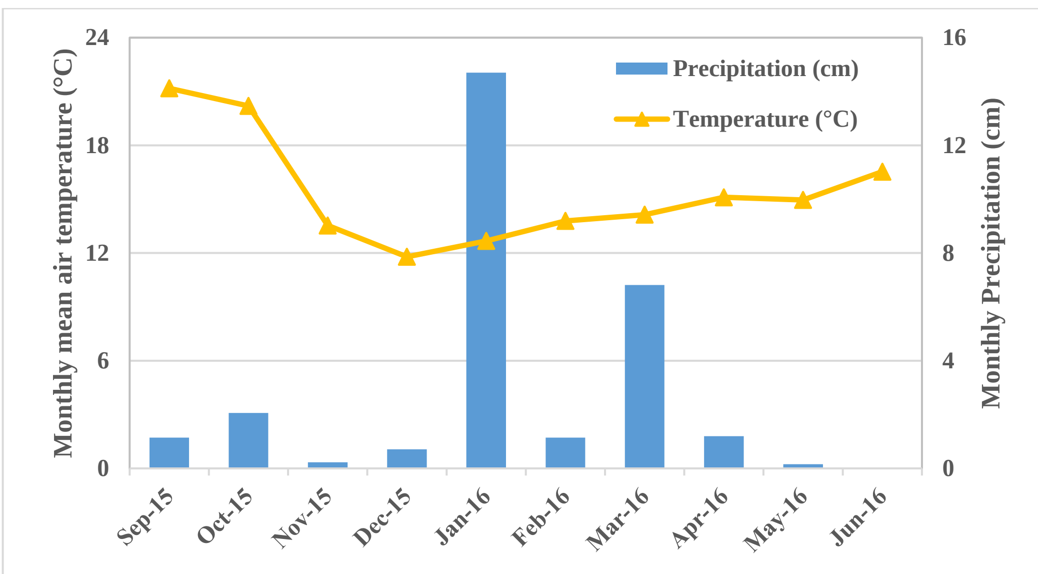


*Figure 1. Climograph of Santa Barbara (Sept 2015 – June 2016); Data source: National Centers for Environmental Information, NOAA; Accessed Dec 8th, 2017.*

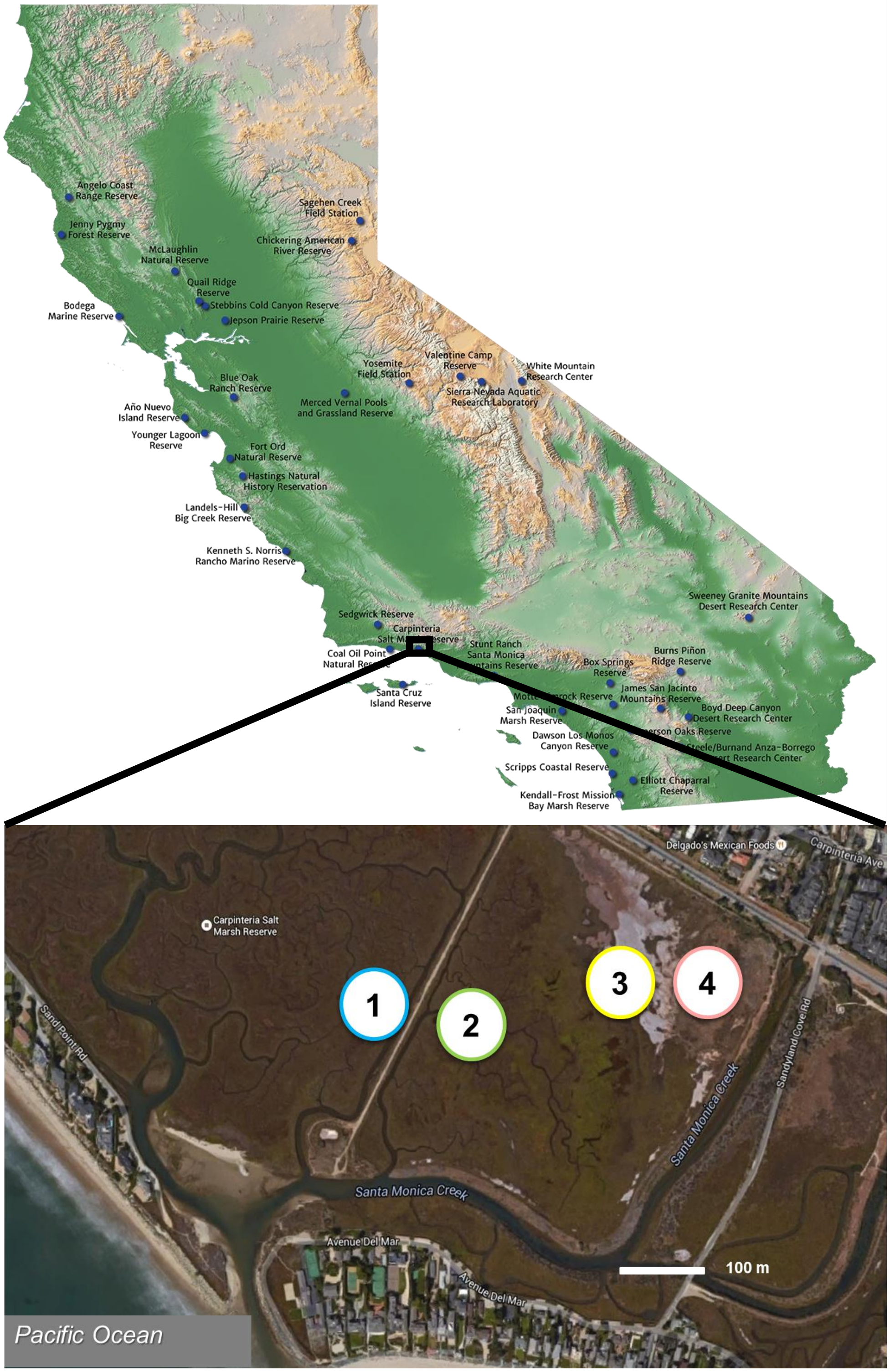


*Figure 2. Location of the Carpinteria Salt Marsh Reserve;*
*Image sources: Google Map http://maps.google.com, retrieved on 12/12/2016;*
*UC CALeDNA: http://www.ucedna.com/reserves-to-visit-1/, retrieved on 12/8/2017.*

*2.2. Gas flux measurements*

Measurements of greenhouse gas exchange were made approximately fortnightly from mid-September 2015 to late May 2016. Twelve plots were established among the four zones described above, with three plots (labeled A, B, and C) approximately 40 to 50 meters apart within each zone. At each plot, exchange of $CO_2$ and $CH_4$ at the surface-atmosphere interface was monitored during low tides using a static dark chamber technique. Twelve aluminum chamber bases were inserted 20 cm into the soils in late August 2015, three weeks before the first measurement, and they remained in the soil throughout the study period. Each base had one Pickleweed plant inside except for the three plots in the mudflat. A channel on the top edge of the base served to hold the chamber in place and to make an airtight seal when filled with water. The chambers are 12.5 L aluminum boxes 25 cm × 25 cm × 20 cm (L × W × H) in dimension. Sampling of the gas within the chamber was carried out with a 30-ml syringe connected to the chamber through two three-way stopcocks and a needle that was inserted through a septum in a small opening on the chamber. The syringe was pumped several times to homogenize the chamber headspace before gas sample collection. A sample of chamber headspace was taken right after the chamber was placed on the base and 20, 40, and 60 minutes after the initial sample. Ambient air samples were also collected at the end of the one-hour interval at 20 cm above ground surface from around each chamber. The syringes were brought back to the laboratory for determination of $CH_4$ and $CO_2$ concentrations within 24 hours after sample collection. Concentrations of $CH_4$ and $CO_2$ were determined on a Shimadzu gas chromatograph (model GC-14A) using helium as a carrier gas, with $CH_4$ analyzed by Flame Ionization Detection (FID) and $CO_2$ by Thermal Conductivity Detection (TCD). Calibrated standards of 1.02, 1.82, and 10 ppmv $CH_4$ (air balanced) and 308, 810, and 1000 ppmv $CO_2$ (nitrogen balanced) from Air Liquide S.A. and

Praxair Technology, Inc. were used to set up a three-point linear regression curve for calibration.

Air temperature at 20 cm above ground surface and soil temperature at 10 cm depth were recorded at each plot during gas sample collection with an Omega® HH506A Multilogger Thermometer. When surface water was present, its salinity was determined with a refractometer (MA887, Milwaukee Instruments, Inc., Rocky Mount, NC, USA). At the end of the study period, aboveground biomass from within each chamber base was harvested, oven dried at 65 °C for 48 hours, and weighed.

At the end of the study period, two intensive field campaigns were carried out to investigate diel patterns of $CH_4$ and $CO_2$ fluxes, especially with regard to the tidal cycle. Flux measurements were made during low tide and high tide and in the middle of the flood tide at the lower marsh zones on May 26, 2016 and at the mudflat and the transition zone on Jun 12, 2016. The sample collections and analyses followed the same procedures as described in this section.

### *2.3. Soil analyses*

Soil cores 50 cm deep were collected from each plot in August 2015 and in June 2016. Around each chamber base, up to 4 cores were extracted and segmented by depth. Soils from the same depth interval were then commingled, sealed in airtight plastic bags, and transported to the laboratory for further analyses.

The soil samples collected in 2015 were cut into 2-cm intervals for the surface 10 cm and into 20-cm intervals for deeper soils, as previous work suggested that the greatest variability of soil properties existed in the surface 10 cm at Carpinteria Salt Marsh (Elgin

2012). The samples were used in the following analyses: estimates of soil organic matter (SOM) content with loss on ignition (LOI) technique at 400 °C for 16 hours, soil pH in one molar potassium chloride solution, and electrical conductivity of saturated paste at 1:2 soil water ratio. In addition, surface soil bulk density was determined by extracting an intact soil core with a metal ring of known volume (67.44 $cm^3$) and oven drying the samples at 105°C for 24 hours.

The soil samples collected in 2016 were cut into three layers: surface 10 cm, 10 – 30 cm, and 30 – 50 cm. They were subsampled for the following analyses: gravimetric soil moisture content (top 10 cm only), soil carbon and nitrogen (C and N) concentrations, and soil particle size analysis (PSA). The gravimetric soil moisture content was calculated as the percent weight loss relative to dry soils after the samples were oven dried for 24 hours at 105°C. The soil C and N concentrations were determined on a Carlo Erba NA 1500 Series 2 Elemental Analyzer with a TCD detector. The C and N samples had passed through 2 mm sieves, were oven dried at 65°C overnight, finely ground to powdery texture, and wrapped in tin capsules (10 mg for soils from the lower marsh zones and 15 mg for soils from the mudflat or the transition zone). Based on soil carbon concentration (%C), soil C content was calculated with the following equation and proper unit conversions:

$$Carbon\ content\ (gC\ m^{-2}) = Bulk\ density \times Depth \times \%C.$$

The PSA was performed following modified pipette technique (Gavlak et al. 2003) which used 0.5% sodium hexametaphosphate (HMP) as dispersant after removal of salts with sodium acetate, soil organic matter with hydrogen peroxide ($H_2O_2$), and iron oxides with sodium dithionite ($Na_2S_2O_4$). Following the pretreatments and 16 hours of horizontal reciprocating shaking, a small fraction of solution with suspended particles was dispensed

10 seconds and 110 minutes after another rigorous shaking by hand. The suspended particles in these two pipette samples supposedly contained soil fractions < 50 μm (silt and clay) and < 2.0 μm (clay only), respectively.

## *2.4. Data handling and statistical analyses*

Gas fluxes were calculated using the slope of a linear fit of $CH_4$ and $CO_2$ concentrations over time, and results were accepted if coefficient of determination ($r^2$) for $CO_2$ was larger than or equal to 0.80. The flux rate was then converted from volume-based to mass-based values following the ideal gas law, corrected for chamber volume and cross-section area and air temperature. The formula for calculating flux rates based on the regression slope is given below (with proper unit conversions):

$$F = \frac{dc}{dt} \times \frac{M}{V_m} \times \frac{V}{A} \times \frac{T_{Lab}}{T_{Field}},$$

where F stands for flux rate (mg $CH_4$ $m^{-2}$ $hr^{-1}$ or mg $CO_2$ $m^{-2}$ $hr^{-1}$); dc/dt the slope of the linear regression for gas concentration gradient through time; M the molecular mass of each gas; $V_m$ the standard molar volume of a gas (22.4 L/mol); V and A the volume and cross section area of the chambers; and $T_{Lab}$ and $T_{Field}$ the absolute air temperatures during lab analysis and fieldwork.

Cumulative $CH_4$ and $CO_2$ emissions were calculated with trapezoidal integration method, as explained in the equation below (with proper unit conversions):

$$E = \sum_{i=1}^{n}[\left(\frac{F_i+F_{i+1}}{2}\right) \times (D_{i+1} - D_i)],$$

where E is the cumulative emissions of $CH_4$ or $CO_2$ (g $CH_4$ $m^{-2}$ or g $CO_2$ $m^{-2}$); n the total number of sampling efforts (n = 19 for Zones 1 and 2; n = 18 for Zones 3 and 4 for the entire study); $F_i$ the flux rate measured from the *i*th sampling day; and $D_i$ the Julian day of the *i*th sampling day (plus 365 for days in 2016). The cumulative $CH_4$ and $CO_2$ emissions were calculated for both the entire 9-month study period (Sept 2015 – May 2016) and every three months, the latter coinciding with northern meteorological seasons (Sept 1st – Nov 30th for fall, Dec 1st – Feb 28th for winter, and Mar 1st – May 30th for Spring). The average daily flux for $CH_4$ and $CO_2$ were obtained from dividing the overall cumulative emissions by the duration of the study ($D_n - D_i + 1 = 259$ days).

To test the statistical significance of the differences among the flux data, analysis of variance (ANOVA) was applied for inter-zone (zone-level) and intra-zone (plot-level) comparisons in both Microsoft Excel and R. Pearson correlation analyses were applied in R to investigate the relationships between the gaseous carbon fluxes and measured environmental variables. For the correlation analyses, individual flux rates from each plot were used with air and soil temperature data, and the average daily fluxes were used with soil moisture, soil texture, soil pH, and SOM data. The values representing soil properties at each plot were depth weighted means, except for moisture content that was only derived from the surface 10-cm soils.

## 3. Results and Discussion

### *3.1. Soil properties and other environmental measurements*

Measurements of physical and chemical properties of surface soils from CSMR had significant variability with contrasts between the two lower marsh zones and the other two zones at higher elevation. When measurements from the lower marsh zone 1 and the lower marsh zone 2 are similar, the two zones are discussed together and simply referred to as the "lower marsh zones". Results from soil measurements are reported in the format of "Mean ± 1 S.D." unless otherwise specified.

### 3.1.1. Soil physical properties

Samples from the lower marsh zones generally had a higher fraction of clay (38 ± 4%) and lower fraction of sand (18 ± 5%) compared to the mudflat (15 ± 5% clay and 46 ± 10% sand) and the transition zone (14 ± 5% clay and 62 ± 19% sand; Figure 3). Most of the soil samples collected from the lower marsh zones were classified as silty clay loam according to the USDA textural soil classification system, and a few as clay loam or silty clay. All soil samples from the mudflat were loam, and all from the marsh-upland transition zone were sandy loam. There was not a clear trend of soil texture variations by depth in the three depth intervals examined: top 10 cm, 10 to 30 cm below surface, and 30 to 50 cm below surface. Further analyses showed that clay fractions tended to have lower coefficients of variation (ratio between the standard deviation and the mean) on the plot and zonal level, which likely had to do with the pipette method we used for PSA. The clay fraction was the only measurement determined directly and was likely less subject to error.

Soil moisture content varied depending on the time of sample collection relative to the tidal regime and precipitation. However, typical values of gravimetric soil moisture were around 54 ± 5.5%, 24 ± 2%, and 13 ± 2.5% for the lower marsh zones, the mudflat, and the upland-transition zone, respectively (Figure 4). The difference in soil moisture content among the zones was largely because lower marsh zones experienced tidal inundation on a daily basis, whereas tidal contribution to soil moisture was limited in the mudflat and rather rare to the surface soils in the transition zone.

Surface soil bulk density ranged from 0.32 ± 0.06 g $cm^{-3}$ for the lower marsh soils to 0.98 ± 0.20 g $cm^{-3}$ for the transition zone and 1.13 ± 0.08 g $cm^{-3}$ for the mudflat (Figure 5). The differences among the zones followed the same pattern as reported by Callaway et al. (1990), but the absolute values from this study were consistently lower by 0.2 to 0.3 g $cm^{-3}$. A synthesis study on marsh soils in Louisiana postulated that the amount of mineral that infiltrates the structural framework formed by organic material determines the soil density for highly organic marsh soils (Gosselink et al. 1984). The lower bulk density of surface soils from the lower marsh zones at CSMR was likely a result of high soil organic content (see “belowSoil chemical properties” below for details) and frequent tidal flushing that drains the mineral components.

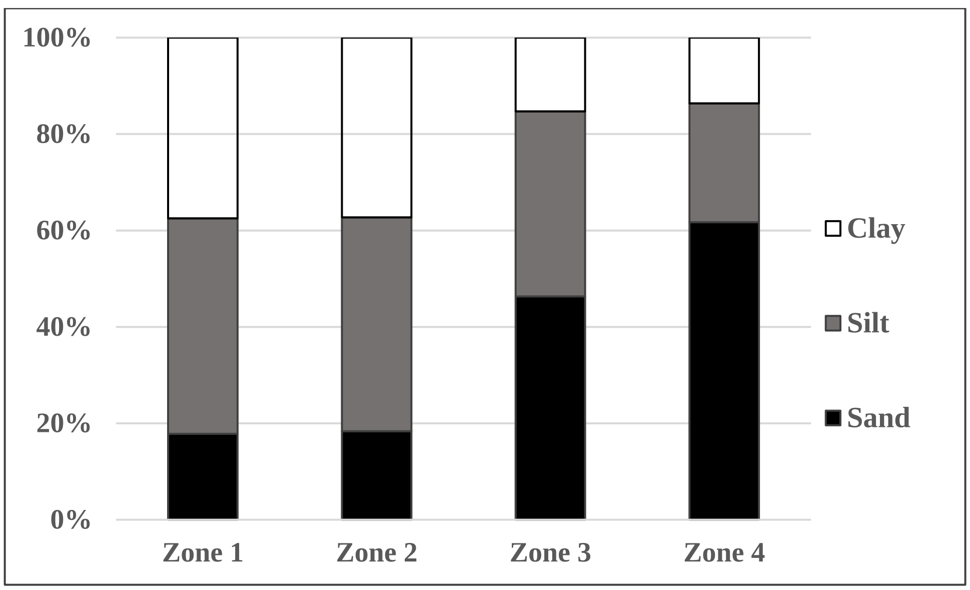


*Figure 3. Depth-weighted soil particle size distribution at CSMR by zone.*

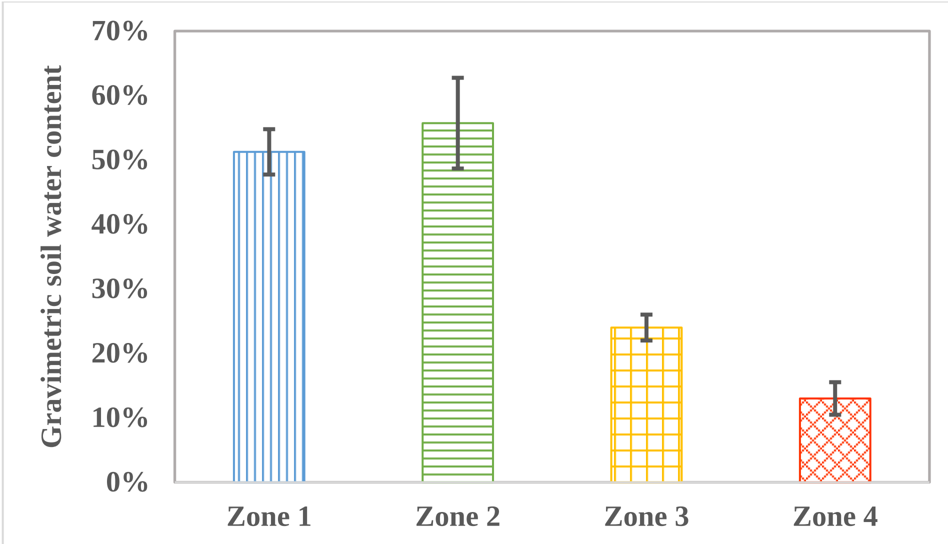


*Figure 4. Gravimetric soil moisture content at CSMR during low tides in May 2016.*

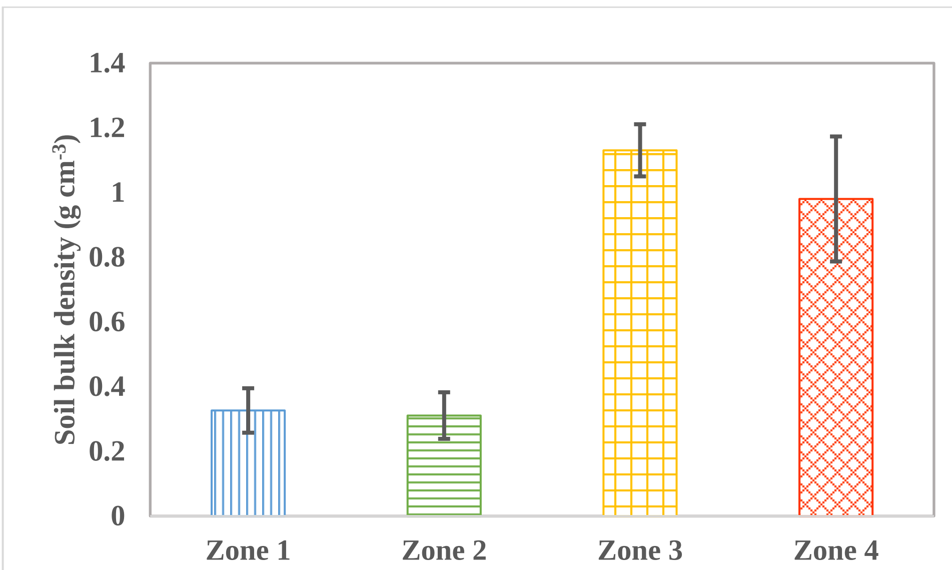


*Figure 5. Surface soil bulk density at CSMR by zone.*

### 3.1.2. Soil chemical properties

The soil carbon and nitrogen concentrations varied with depth within each zone and from one zone to another. Soil carbon and nitrogen concentrations were higher for samples collected at the surface than those from greater depths except for the mudflat. The surface soils (0 – 10 cm) typically had 50% more carbon and nitrogen than soils 30 – 50 cm deep in the lower marsh zones on a per unit mass basis, and the difference was largest in the marsh-upland transition zone where soil carbon and nitrogen concentrations were both 2- to 4-fold greater at the surface. There was no significant variation with depth for samples from the mudflat.

Across the wetland zones, the lower marsh zones had carbon concentration ranging from 2.6% to 4.7%, the mudflat 0.8% to 1.5%, and the transition zone 0.3% to 2.2%. The nitrogen concentration ranged from 0.23% to 0.40% for the lower marsh zones, 0.05% to 0.10% for the mudflat, and 0.04% to 0.20% for the transition zone. Generally, soils from the lower marsh zones had three to four times greater carbon and nitrogen concentration compared to soils from the mudflat or the transition zone (Table 1). The observation was also compatible with the soil organic matter measurements as shown in Figure 6 even though LOI measurement of soil organic matter tends to overestimate the SOM content by including some structural water loss as oxidized organic matter.

When bulk density is taken into account, the surface soil carbon content in each zone showed a different pattern. The transition zone had the highest carbon content (1.89 ± 0.35 kg C $m^{-2}$), followed by the lower marsh zones (1.29 ± 0.13 kg C $m^{-2}$ and 1.46 ± 0.27 kg C $m^{-2}$). Although the mudflat still had the lowest carbon content among all the zones (1.89 ± 0.09 kg C $m^{-2}$), the difference was considerably smaller.

Interestingly, the soil carbon to nitrogen ratio (C/N) remained relatively constant throughout the lower marsh, ranging from 10.4 to 12.6 regardless of the depth; C/N was more variable for samples from the mudflat (10 to 25) and the transition zone (7 to >50). On average, however, the mudflat had the highest C/N (≈ 14) compared to the lower marsh zones (C/N ≈ 11.5 to 12) and the transition zone (C/N ≈ 11).

*Table 1. CSMR soil carbon and nitrogen concentrations by zone.*

| | %C | | %N | |
|---|---|---|---|---|
| | **Mean** | S.D. | **Mean** | S.D. |
| Zone 1 | **3.28** | 0.27 | **0.28** | 0.02 |
| Zone 2 | **3.79** | 0.38 | **0.32** | 0.02 |
| Zone 3 | **1.02** | 0.31 | **0.07** | 0.02 |
| Zone 4 | **0.97** | 0.21 | **0.09** | 0.01 |

Higher carbon and nitrogen concentrations at the surface in the lower marsh zones and the transition zone, as well as the absence of such pattern in the mudflat, suggests that vegetation is the dominant contributor to soil carbon and nitrogen content. Consistent with findings in literature (Chmura et al. 2003), high primary productivity combined with slow decomposition rates due to frequent inundation allows for accumulation of soil organic matter in the lower marsh zones.

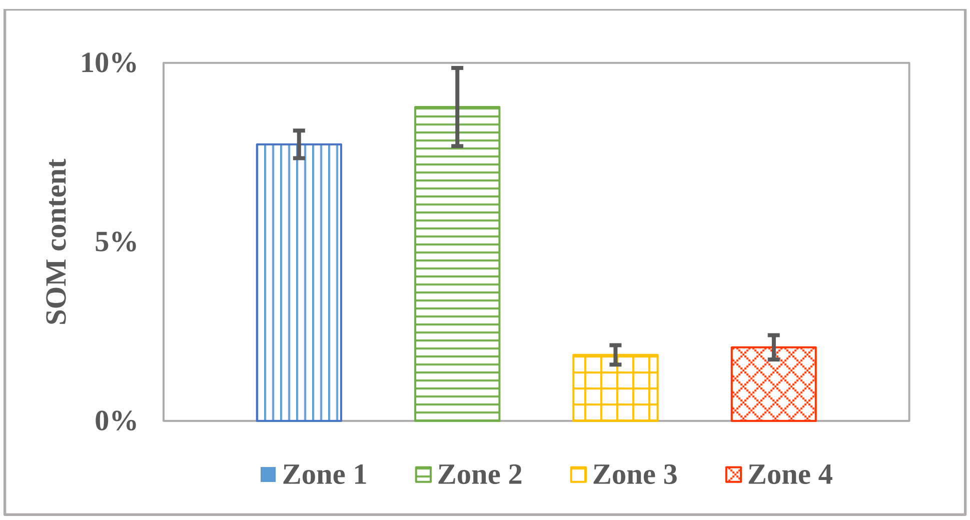


*Figure 6. CSMR soil organic matter content (top 50 cm) by zone as determined by loss-on-ignition method; error bars representing values of one standard deviations in each zone.*

There was a significant difference (p-value < 0.001) in soil pH between soils in the lower marsh zones and the other two zones. Soil samples from the lower marsh zones were slightly acidic, with average pH values of 6.6 and 6.5. Soils from the mudflat and the transition zone were slightly alkaline, with pH values of 8.2 and 7.9, respectively. The soil pH values at CSMR were similar to those found in other coastal salt marshes (Álvarez Rogel et al. 2001; Yuan et al. 2014; Martin and Moseman-Valtierra 2015). For all four zones, there was not a clear pattern of soil pH variations with depth. The lower pH values in lower marsh zones were likely attributable to high soil organic matter content that could release $H^+$ ions associated with organic anions. The higher pH in mudflat and transition zones was likely linked to carbonate accumulation related to infrequent tidal inundation and capillary rise of groundwater followed by rapid water evaporation and salt deposition.

#### 3.1.3. Other environmental measurements

The aboveground biomass within each chamber at the end of the study period was consistent across zones (0.3 to 0.4 $kg/m^2$) with some exceptions in the lower marsh zones. Destructive sampling of biomass was not possible during the study, and most vegetation was dead at the time of harvest (June 2016), except for plot 1A. The plant species composition at the three plots in the transition zone had changed from predominantly Pickleweed to a mixture of Pickleweed and more upland species by the time of harvest.

Salinity of waters at the soil surface in the lower marsh zones typically ranged between 32 to 38 g/L and occasionally exceeded 50 g/L, indicating that the major water source was seawater. When water was present in the mudflat, the salinity values were typically above 35 g/L and could occasionally go above 70 g/L. The higher surface water salinity in the mudflat corroborates the claim that the mudflat is less tidally connected and is evaporation dominated. On a finer spatial scale, that Plot 1A tended to have 3 to 5 g/L higher salinity than the other locations in the lower marsh matches well with its soil texture and $CH_4$ and $CO_2$ fluxes (see "Intra-zone variations" for detailed discussions).

### *3.2. Spatial and temporal patterns of $CH_4$ fluxes*

The $CH_4$ fluxes from the Carpinteria Salt Marsh had significant ($p = 0.072 < 0.1$) spatial variability on the zonal level (Table 2). The average daily $CH_4$ flux rates from the lower marsh zones (2.2 ± 1.4 mg $CH_4$ $m^{-2}$ $d^{-1}$ and 1.9 ± 0.2 mg $CH_4$ $m^{-2}$ $d^{-1}$) surpassed those from the mudflat (0.25 ± 0.06 mg $CH_4$ $m^{-2}$ $d^{-1}$) by an order of magnitude, and the marsh-upland transition zone was a net methane sink (-0.07 ± 0.12 mg $CH_4$ $m^{-2}$ $d^{-1}$). The $CH_4$ fluxes were temporally heterogeneous, and no consistent pattern on a seasonal scale was observed at the zone level (p values of ANOVAs equal 0.44, $1.5\times10^{-5}$, 0.0053, and 0.71 for Zones 1, 2, 3, and 4, respectively).

$CH_4$ fluxes from the lower marsh zones 1 and 2 were comparable to the $CH_4$ fluxes from other polyhaline salt marshes (salinity > 18 g/L) with 1 ± 2 g $CH_4$ $m^{-2}$ $yr^{-1}$ methane flux (Poffenbarger et al. 2011). Poffenbarger et al. (2011) summarized 31 observations in tidal marshes (excluding mangroves) where salinity ranged from below 0.5 g/L to above 18 g/L and found a negative relationship between pore water salinity and methane flux. Bridgham et al. (2006) used 1.3 g $CH_4$ $m^{-2}$ $yr^{-1}$ (n = 25, 1 SE = 3.3) for estuarine wetlands in their modeling of the carbon balance of North American wetlands. A few studies that were not included in Poffenbarger et al. (2011) or Bridgham et al. (2006) showed a wider range of $CH_4$ flux rates from similar ecosystems. Two adjacent salt marshes with soil salinities greater than 20 g/L along the Atlantic coast of Canada had $CH_4$ flux rates of 0.5 ± 1.4 mg $CH_4$ $m^{-2}$ $d^{-1}$ at the site with 0–2 m tidal range (similar to CSMR) and 0.05 ± 0.62 mg $CH_4$ m-

$^{2}$ $d^{-1}$ at the site with > 4 m tidal range (Chmura et al. 2011). Three coastal marshes along a salinity gradient within the Mobile Bay Estuary, Alabama, had mean daily $CH_4$ emissions of 28.8 ± 9.6, 14.4 ± 8.4, and 15.6 ± 2.4 mg $CH_4$ $m^{-2}$ $d^{-1}$, all significantly higher than the lower marsh zones at CSMR (2.2 ± 1.4 and 1.9 ± 0.2 mg $CH_4$ $m^{-2}$ $d^{-1}$, respectively). Results from other studies were less comparable due to differences in tidal conditions, salinity level, and/or $CH_4$ reservoirs (e.g., water – air $CH_4$ exchange instead of sediment/vegetation – air exchange).

*Table 2. Estimates of annual $CH_4$ flux rates from different zones at CSMR.*

| Zones | Mean (g $CH_4$ $m^{-2}$ $yr^{-1}$) | S.D. (g $CH_4$ $m^{-2}$ $yr^{-1}$) |
|---|---|---|
| Lower Marsh Zone 1 | 0.81 | 0.5 |
| Lower Marsh Zone 2 | 0.69 | 0.1 |
| Mudflat | 0.09 | 0.02 |
| Marsh-upland Transition | -0.03 | 0.04 |

### 3.2.1. Environmental influences on $CH_4$ fluxes

The distinct variations in the methane flux rates from each zone correlated well with soil properties, although correlation does not imply causal relationships. For example, there was a negative correlation between cumulative methane fluxes from each plot and the soil pH ($r$ = -0.78, p = 0.0031 < 0.01). However, the pH values of the soil samples from the Carpinteria Salt Marsh Reserve largely fell within the range of 6 to 8, which is the optimum for most methanogens (Dunfield et al. 1993; Garcia et al. 2000; Le Mer and Roger 2001). Thus, the correlation observed here highlights the spatial variability of methane emissions and soil pH by zone, and not necessarily mechanistic control on methane emissions by soil pH.

There was a positive correlation between cumulative methane fluxes and soil carbon concentration (*r* = 0.74, $p = 0.0055 < 0.001$; Figure 7). Given that the methane fluxes examined here represent the net balance between methanogenesis and methanotrophy at the interface between the marsh surface and the atmosphere, this correlation between methane fluxes and soil C concentration is consistent with carbon availability possibly limiting $CH_4$ production. Other things being equal, the high organic carbon content in the lower marsh soils would allow greater methane production compared to the other zones where less soil carbon was available. The effect of soil carbon content on methane production has also been documented in previous studies. It was postulated that an increase in carbon input can boost overall heterotrophic microbial respiration, which also favors methanogenic respiration, as more of the competitive electron acceptor supply is consumed (Sutton-Grier and Megonigal 2011). Wachinger et al. (2000) analyzed the structure of soil cores with tomography at 1-mm resolution and demonstrated that the distribution of fresh organic material is correlated to methanogenic archaea population size and is the most dominant factor for the spatial variation in $CH_4$ production on the micro-scale. Yuan et al. (2014) reported significant ($p < 0.05$) correlations between soil $CH_4$ production potential and the concentrations of soil organic carbon as well as the abundance of methanogenic archaea for a *Spartina alterniflora* invasion chronosequence. Interestingly, the soil $CH_4$ production potential was not significantly correlated to dissolved organic carbon in their study. Besides the quantity of SOM, sometimes soil C/N ratios could be used as indicators for the quality of SOM and its decomposability, as lower C/N ratios could lead to increased microbial activity and consequently a higher content of organic precursors for methanogenesis in soil solutions (Fiedler and Sommer 2000). According to Fiedler and Sommer (2000), wetland soils with a

C/N ratio of 11 had much higher methane emissions compared to soils with a C/N ratio of 17. We did not observe a similar pattern in this study between soil C/N ratios and $CH_4$ fluxes, likely because the soil C/N ratios were not sufficiently different among zones, and the absolute soil carbon content was likely a stronger driver of the $CH_4$ patterns.

The cumulative methane fluxes and soil particle size distribution correlated well. The correlation coefficients between cumulative $CH_4$ fluxes and sand, silt, and clay were -0.81, +0.70, and +0.79 ($p < 0.05$; see also Figure 8), respectively. In contrast, the correlation coefficients between cumulative $CO_2$ fluxes and sand, silt, and clay fractions were only +0.21, -0.51, and +0.06 ($p > 0.05$). The negative correlation between methane fluxes and sand fractions could be attributed to sand having larger pore space and allowing better aeration and faster drainage, thus contributing to suppressing methanogenesis and encouraging methane oxidation. A larger clay fraction could improve water retention and be more conducive to maintaining low redox potential suitable for methanogenesis. Previous studies have reported varying correlations between methane fluxes and soil texture. Results from an incubation study with Elbe River marshland soils and artificially textured model soils under oxic and subsequent anoxic conditions showed that the methane production rates increased in the sequence of increasing clay fractions: sand < gravel < clayey silt (marshland soil) ≤ clay (Wagner et al. 1999). These researchers attributed the pattern to the large surface area and the amount of negative charges that finer soil particles and organic matter provided for the sorption of microorganisms and nutrients, which protect methanogens from oxygen and result in higher $CH_4$ production. Le Mer and Roger (2001) reviewed a few studies on methane emissions from rice fields and concluded that high clay contents may sometimes impede methane ebullition and that some soil types and clay mineralogy can protect organic matter from mineralization and delay methanogenesis.

There was a positive correlation between soil moisture content and cumulative methane fluxes ($r = 0.76$, $p = 0.0044 < 0.01$) from Carpinteria Salt Marsh Reserve. Similar patterns have been reported from forest ecosystems (e.g., Lessard et al. 1994; Itoh et al. 2012; Christiansen et al. 2016) where soil moisture may exert a dominant role on variability, magnitude, and direction of $CH_4$ fluxes. High soil moisture content has been found to suppress methanotrophy, especially when soil water content is near or above field capacity (Czepiel et al. 1995; Le Mer and Roger 2001). Soil moisture was negatively correlated with redox potential in a Yangtze River estuarine wetland (Bu et al. 2015), and low redox conditions are more favorable for methanogenesis. It is important to recognize that soil moisture content is tightly linked to tidal cycles and is consequently temporally variable in coastal salt marshes. That the lower marsh zones at Carpinteria Salt Marsh Reserve had higher $CH_4$ fluxes with possible salinity suppression of methanogenesis highlights the importance of soil moisture on methane dynamics.

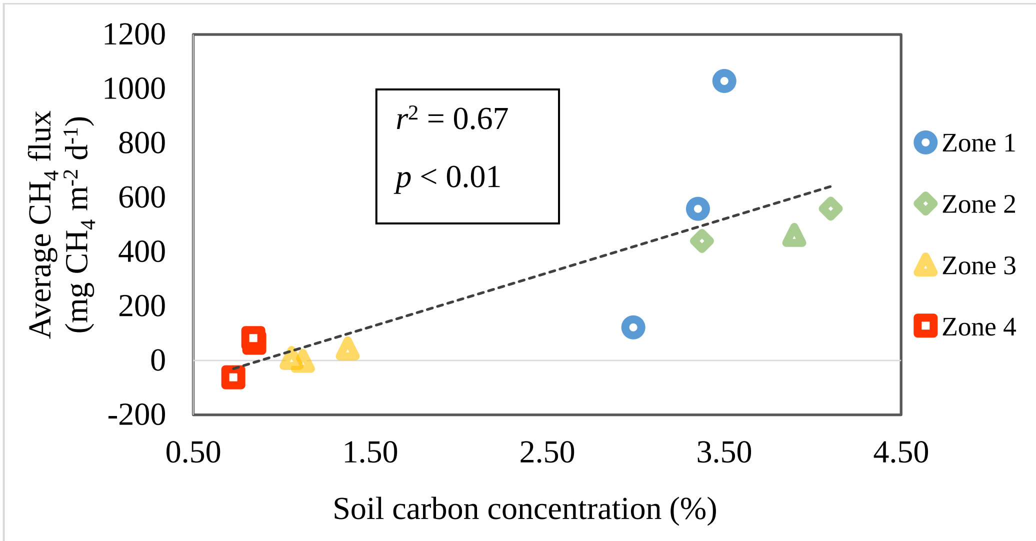


*Figure 7. Correlation between average $CH_4$ flux and soil carbon concentration at CSMR.*

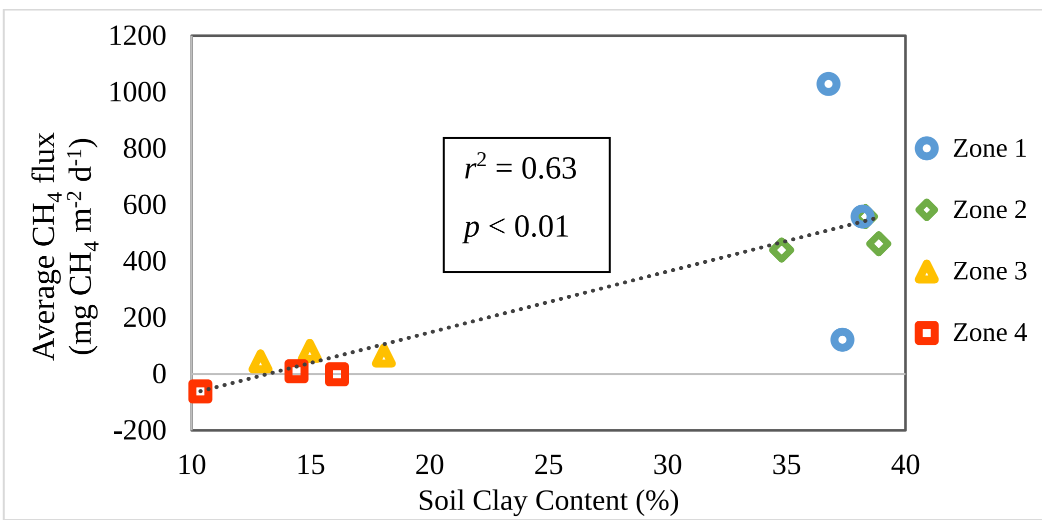


*Figure 8. Correlation between average $CH_4$ flux and soil clay content at CSMR.*

### *3.3. Spatial and temporal patterns of $CO_2$ fluxes*

The $CO_2$ fluxes had significant ($p = 5.6\times10^{-5} < 0.001$) spatial variability. Averaged over the study period (Sept 2015 – June 2016), the marsh-upland transition zone had the highest $CO_2$ flux rates at 3.7 ± 0.5 g $CO_2$ $m^{-2}$ $d^{-1}$, followed closely by the lower marsh zones (2.7 ± 0.4 g $CO_2$ $m^{-2}$ $d^{-1}$ and 2.0 ± 0.5 g $CO_2$ $m^{-2}$ $d^{-1}$), which were one order of magnitude higher than the $CO_2$ fluxes from the mudflat (0.3 ± 0.05 g $CO_2$ $m^{-2}$ $d^{-1}$). $CO_2$ fluxes also showed significant temporal variability on a seasonal scale within each zone ($p < 0.05$; Figure 9). During the three-month period in winter, the $CO_2$ flux rates from each zone were less than half the magnitudes of the other two periods, with Zone 4 being an exception. Curiously, the marsh-upland transition zone started with only moderate $CO_2$ fluxes (177 ± 18 mg $CO_2$ $m^{-2}$ $hr^{-1}$) compared with the lower marsh zones (218 – 554 mg $CO_2$ $m^{-2}$ $hr^{-1}$) at the beginning of the study period. However, the fluxes in the transition zone exceeded those from the other zones accompanying a shift in plant species composition (based on personal observation) starting in Feb 2016. By the end of the study period, the transition zone had consistently higher $CO_2$ flux rates (238 ± 15 mg $CO_2$ $m^{-2}$ $hr^{-1}$) than the other zones (30 – 183 mg $CO_2$ $m^{-2}$ $hr^{-1}$). Estimates of $CO_2$ flux rate from each zone are summarized in Table 3; for ease of comparison with other studies, the values are presented as $CO_2$ fluxes by hour, by day, and by year, respectively.

*Table 3. Estimates of $CO_2$ flux rate from different zones at CSMR.*

| | By hour (Mean ± S.D.) | By day (Mean ± S.D.) | By year (Mean ± S.D.) |
|---|---|---|---|
| *Zone 1* | 117 ± 30 mg $CO_2$ $m^{-2}$ $hr^{-1}$ | 3 ± 1 g $CO_2$ $m^{-2}$ $d^{-1}$ | 1021 ± 259 g $CO_2$ $m^{-2}$ $yr^{-1}$ |
| *Zone 2* | 159 ± 26 mg $CO_2$ $m^{-2}$ $hr^{-1}$ | 4 ± 1 g $CO_2$ $m^{-2}$ $d^{-1}$ | 1395 ± 227 g $CO_2$ $m^{-2}$ $yr^{-1}$ |
| *Zone 3* | 18 ± 3 mg $CO_2$ $m^{-2}$ $hr^{-1}$ | 0.4 ± 0.1 g $CO_2$ $m^{-2}$ $d^{-1}$ | 159 ± 24 g $CO_2$ $m^{-2}$ $yr^{-1}$ |
| *Zone 4* | 219 ± 29 mg $CO_2$ $m^{-2}$ $hr^{-1}$ | 5 ± 0.7 g $CO_2$ $m^{-2}$ $d^{-1}$ | 1921 ± 250 g $CO_2$ $m^{-2}$ $yr^{-1}$ |

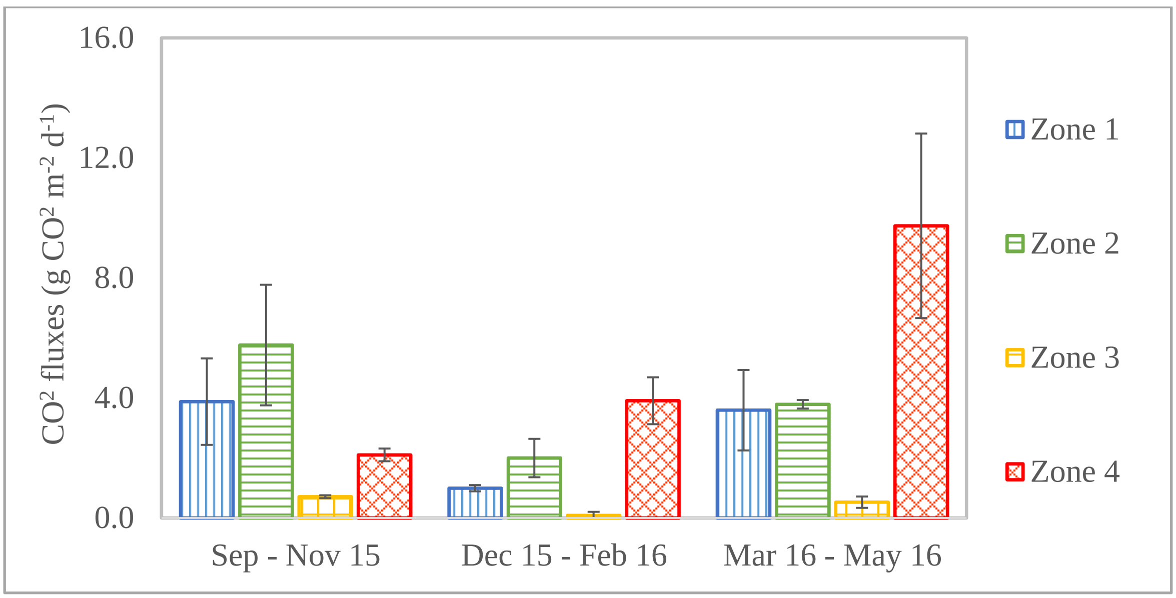


*Figure 9. Carbon dioxide fluxes from different zones at CSMR during three three-month periods (boundaries included).*

The $CO_2$ fluxes from Carpinteria Salt Marsh Reserve are comparable to the $CO_2$ fluxes from similar ecosystems. For salt marshes within the coterminous United States, many studies have been focused along the Atlantic Coast. Three coastal marshes along a salinity gradient in a northern Gulf of Mexico estuary had annual ecosystem respiration rates of 2104, 1032, and 1066 g $CO_2$ $m^{-2}$ $yr^{-1}$ (Wilson et al. 2015). Magenheimer et al. (1996)

reported that there was no significant difference in $CO_2$ flux among the plant communities at a macrotidal salt marsh in the Bay of Fundy. Their observed $CO_2$ fluxes (2.2 – 2.8 g $CO_2$ $m^{-2}$ $d^{-1}$) represented community respiration without photosynthesis and were negatively correlated with water table position and positively correlated with aboveground biomass, but not with salinity. Nighttime $CO_2$ fluxes ranged between 174 and 630 mg $CO_2$ $m^{-2}$ $hr^{-1}$ from Sage Lot Pond within the Waquoit Bay National Estuarine Research Reserve (Moseman-Valtierra et al. 2016), which were slightly higher than the $CO_2$ fluxes from the lower marsh zones and the transition zone at CSMR. Similar pattern of slightly higher $CO_2$ flux rates than that from CSMR but on the same order of magnitude ($10^2$ – $10^3$ mg $CO_2$ $m^{-2}$ $hr^{-1}$) was also reported in Canada (Chmura et al. 2011) and China (Xu et al. 2014). Studies that used transparent chambers or floating chambers or focused on types of wetlands other than coastal salt marshes were not included in this comparison.

#### 3.3.1. Environmental influences on $CO_2$ fluxes

$CO_2$ fluxes were positively correlated with soil temperature in some parts of the CSMR, but the strength of correlation and its statistical significance varied by zone. There was a positive correlation between soil temperature and $CO_2$ fluxes from the lower marsh zones. The linear coefficient of determination values ($r^2$) were 0.33 and 0.52 for Zone 1 and 2, respectively, and 0.42 when the data for both zones were analyzed together (p-value < 0.01 for all cases). Exponential curves provided better fit for both ($r^2$ = 0.50 and 0.59), which is not surprising, as $CO_2$ production is a predominantly biological process and rises with an increase in temperature. The data suggest that the $CO_2$ fluxes from the lower marsh zones were influenced by root and microbial respiration, which in turn was likely controlled by soil temperature that regulated enzymatic activities.

The mudflat had a positive correlation between soil temperature and $CO_2$ fluxes ($r^2$ = 0.21, $p < 0.05$), although there were notable differences compared to the lower marsh zones. The mudflat consistently had higher soil temperatures but the overall magnitude of $CO_2$ fluxes was less than 20% of that from the lower marsh. The warmer soil temperature could be attributed to lower soil water content and lack of vegetation cover. The lower soil $CO_2$ fluxes were likely the result of high soil bulk density and low carbon content. In addition, the mudflat was prone to waterlogged conditions due to ineffective drainage as evidenced by high surface water salinity, especially during perigean spring tides in winter months, which would suppress aerobic respiration.

There was no significant correlation between soil temperature and $CO_2$ fluxes from the marsh-upland transition zone ($r^2$ = 0.002, $p >> 0.05$). This suggests that belowground heterotrophic respiration was not the dominant contributor to $CO_2$ fluxes from this area.

Correlations between temperature and ecosystem respiration have been observed in other salt marsh ecosystems. Wilson et al. (2015) reported significant positive correlations between both soil and air temperatures and ecosystem respiration at three salt marshes within the Mobile Bay Estuary, Gulf of Mexico, and they were able to model changes in ecosystem respiration under warming scenarios. Similar to the patterns observed at the CSMR, Xu et al. (2014) reported a contrast in $CO_2$ fluxes from a coastal saline wetland in southeast China between growing season and non-growing season, and they found that the mean $CO_2$ fluxes from the tidal flats with different plant communities all showed positive correlations with air temperature.

The $CO_2$ flux rates from CSMR were also likely influenced by vegetation. First, the presence of vegetation contributed to significantly higher $CO_2$ fluxes from the lower marsh zones and the transition zone compared to the mudflat. There was a positive correlation between the aboveground biomass at the end of the study period and $CO_2$ flux rates ($r$ = 0.701, $p < 0.05$). The mudflat could not support vegetation growth due to high soil salinity. Therefore, its $CO_2$ fluxes were primarily produced by microbial respiration in the mudflat and were consistently lower than the other zones. Second, anecdotal evidence suggested that the phenology and types of vegetation might be an important determinant of the magnitude of $CO_2$ fluxes. Pickleweed (*Sarcocornia pacifica*) predominated the transition zone at the beginning of the study period when it had a competitive advantage in the dry, compact, and somewhat saline soil. The $CO_2$ fluxes from the transition zone at this stage were moderate and slightly lower than the lower marsh zones. However, more upland species (such as *Senecio vulgaris* and *Lolium multiflorum*) started to emerge in late winter and cohabited with Pickleweed until the end of the study period. Correspondingly, the $CO_2$ fluxes from the transition zone started to exceed $CO_2$ fluxes from the lower marsh zones, usually by 2- to 3-fold, due to increased autotrophic respiration. The effect of plant phenology and species transition can also be seen where bifurcation of $CO_2$ fluxes at higher air temperature (> 18 ℃) corresponded to data collected before and after the appearance of upland species in the transition zone (Figure 10). Similar trend was also observed at other plots in the transition zone, but the data are not shown here to preserve visibility.

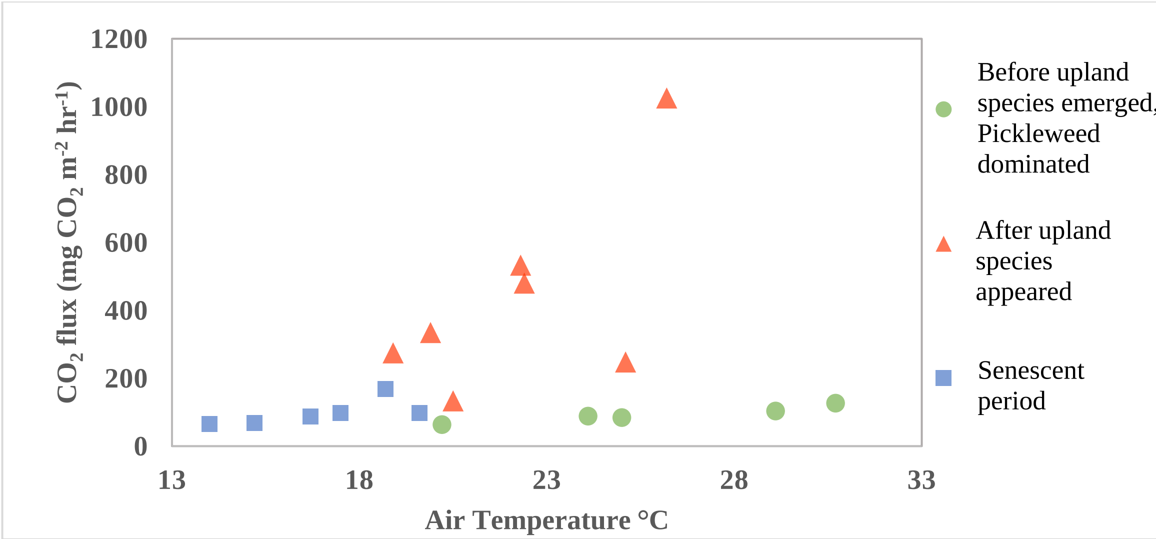


*Figure 10. Carbon dioxide flux from plot 4C vs. air temperature.*

### *3.4. Intra-zone variations*

In addition to the differences observed among zones, there were considerable variations within each zone in terms of soil properties and gas fluxes. For instance, Plot 1A was located about two meters to the east of a side channel and had consistently higher sand fractions at each depth interval compared to the other two plots in the same zone (Table 4). The texture data from this plot was excluded from the overall lower marsh zones soil texture data reported earlier.

*Table 4. Sand fractions of soils at different depths from the lower marsh zone 1, CSMR.*

| Depth interval | 1A | 1B | 1C |
|---|---|---|---|
| **0 – 10 cm** | 26 (4) | 17 (2) | 18 (1) |
| **10 – 30 cm** | 27 (5) | 10 (1) | 15 (2) |
| **30 – 50 cm** | 62 (2) | 10 (1) | 20 (1) |

The higher sand fraction in this plot was likely the result of cumulative deposition of coarse soil particles along channel banks after flood events. A similar pattern has been observed in other coastal wetlands (Yu et al. 2015) and can be attributed to reduced transport of soil particles by water as particle size increases. The higher sand fractions in the soil have important implications for gas exchange, as sand allows for faster tidewater drainage and better aeration, which would increase oxygen availability and be more conducive to aerobic respiration and methane oxidation. In fact, the $CO_2$ flux from plot 1A was the highest within lower marsh zone 1, and the $CH_4$ flux was the lowest among all plots in the lower marsh zones (Table 5). There were also a few cases of negative $CH_4$ fluxes at Plot 1A, which indicate net methane uptake.

*Table 5. $CH_4$ and $CO_2$ flux rates from individual plots in the lower marsh zones.*

| Plot | 1A | 1B | 1C | 2A | 2B | 2C |
|---|---|---|---|---|---|---|
| $CH_4$ fluxes (mg $CH_4$ $m^{-2}$ $d^{-1}$) | 0.47 | 2.15 | 3.97 | 1.70 | 1.78 | 2.16 |
| $CO_2$ fluxes (g $CO_2$ $m^{-2}$ $d^{-1}$) | 3.64 | 2.82 | 1.91 | 3.82 | 4.55 | 3.04 |

Microtopography is another aspect that contributes to the intra-zone variations in soil properties and gas fluxes. Field observations confirmed that small variations in surface elevation within the lower marsh zones could influence the tidal inundation frequency and duration. Thus, two adjacent spots within the same lower marsh zone might provide different microenvironments. For example, prolonged exposure (absence of inundation) could be caused by a small elevation increase, especially during neap tides. Similarly, alternative electron acceptors (e.g., sulfate) could be replenished by tidewater at different frequencies, whereas low redox potential could be maintained by micropores in soils with high clay content. The heterogeneity in soil properties and other environmental conditions offers microsites for various biogeochemical reactions and serves as the basis for intra-zone variations in $CH_4$ and $CO_2$ fluxes from the lower marsh surface.

Intra-zone variations were manifested at the mudflat and at the marsh-upland transition zone. Plot 4C in the marsh-upland transition zone was the furthest from the ocean and had the highest elevation. It consistently had the lowest soil moisture content and the lowest clay fractions among all plots; the soil carbon and nitrogen concentrations were also the lowest. This site was the largest sink of methane (-0.24 mg $CH_4$ $m^{-2}$ $d^{-1}$) among all plots, and it had the highest $CO_2$ flux rate (6.21 g $CO_2$ $m^{-2}$ $d^{-1}$).

In summary, heterogeneity in edaphic properties and gaseous carbon emissions exists at different spatial scales in Carpinteria Salt Marsh Reserve. Zones represent different environmental factors (e.g., soil texture, tidal regime) related to $CH_4$ and/or $CO_2$ emissions. Within each zone, these factors also vary.

### *3.5. Tidal fluctuations and gas fluxes from soil*

To investigate the potential effects of tidal flushing on $CH_4$ and $CO_2$ fluxes from CSMR, we conducted two field campaigns at the end of the regular study period during which fluxes at low tide, flood tide, and high tide were measured. On the zonal level, the overall trend was that both $CH_4$ and $CO_2$ fluxes increased with the inflow of flood tide at the lower marsh zones (Table 6). On the plot level, $CH_4$ and $CO_2$ fluxes from all plots but one ($CH_4$ fluxes from Plot 2A) were smaller during low tide than during high tide. Plot 1A had negative $CH_4$ fluxes, and the magnitude of the negative fluxes increased as tide level rose, suggesting greater $CH_4$ uptake. In contrast, no such trend was present in the mudflat or the transition zone, where no direct tidal influence was observed during the 8-hour period of measurements. It is worth noting that all previous flux data from the lower marsh zones were obtained within two hours before or after low tide, as this period was the only time with access to the study site. This could potentially lead to an underestimate of the cumulative fluxes for both $CO_2$ and $CH_4$ from the lower marsh zones.

*Table 6. $CH_4$ and $CO_2$ fluxes from the lower marsh zones at different tidal stages.*

| | | $CH_4$ fluxes (µg $CH_4$ $m^{-2}$ $hr^{-1}$)<br>Mean ± Standard error | $CO_2$ fluxes (mg $CO_2$ $m^{-2}$ $hr^{-1}$)<br>Mean ± Standard error |
|---|---|---|---|
| Zone 1 | Low tide | 15 ± 8 | 223 ± 90 |
| | Flood tide | 20 ± 13 | 220 ± 73 |
| | High tide | 30 ± 19 | 309 ± 113 |
| Zone 2 | Low tide | 5 ± 4 | 177 ± 92 |
| | Flood tide | 10 ± 6 | 215 ± 42 |
| | High tide | 13 ± 3 | 267 ± 87 |

Bubbling, i.e., ebullition, from both lower marsh zones during flood tide and high tide, was observed and could contribute to higher gas fluxes. The static chamber technique used in this study cannot separate the contribution of ebullition from the overall fluxes. However, Middelburg et al. (1996) have demonstrated that *in situ* measurements of $CO_2$ and $CH_4$ concentrations in chambers with photoacoustic infrared detection technique may distinguish ebullitive $CH_4$ fluxes from diffusive fluxes, as ebullition would cause an abrupt increase in $CH_4$ concentrations. In their study at the Westershelde Estuary, The Netherlands, ebullition rates were high immediately following tidal exposure at low tide and just before inundation, which was attributed to a change in pore space pressure during tidal events. A similar pattern was documented in the tidal freshwater portions of the White Oak River estuary, although ebullition rates were sometimes higher immediately after the tidal minimum, i.e., during flood tide (Chanton et al. 1989). Ebullition induced by the flood tide could be linked to sediment matrix expansion due to reduced effective stress and increased pore fluid pressure as demonstrated by laboratory measurements and model simulations (Chen and Slater 2016). These results suggest that tidal flushing, regardless of flood tide or ebb tide, may be associated with increased gas fluxes from the soil.

## 4. Conclusions and Implications

Average $CH_4$ fluxes from Carpinteria Salt Marsh Reserve ranged between -0.03 and 0.81 g $CH_4$ $m^{-2}$ $yr^{-1}$. These measurements are consistent with previous studies of polyhaline wetlands and are low compared to mesohaline, freshwater, or oligohaline wetlands. Contrary to the original hypothesis, there was significant spatial variability among the lower marsh zones, the mudflat, and the marsh-upland transition zone at CSMR in terms of $CH_4$ fluxes, which correlated well with most edaphic properties in each zone.

The average $CO_2$ flux rates from CSMR ranged between 159 to 1921 g $CO_2$ $m^{-2}$ $yr^{-1}$, which were comparable to those from other salt marsh ecosystems. $CO_2$ fluxes showed no correlation with most soil properties, except for soil temperatures, although the correlations between $CO_2$ fluxes and air and soil temperatures were zone dependent. The findings suggest that there was considerable spatial and temporal variability in $CO_2$ emissions with regard to both season and salt marsh zonation.

This study provides new data on gaseous carbon fluxes in Pacific coastal wetlands and sheds light on biogeochemistry of coastal marshes in a Mediterranean climate. It highlights the diverse and dynamic nature of salt marsh biogeochemistry on seasonal and diurnal scales within and across different zones. Findings from this study have implications for coastal wetland management and conservation practices. With global climate change, a small alteration in relative marsh surface elevation due to sea level rise or changes in carbon sequestration rate may lead to significant changes in its tidal regime and a gradual shift in salt marsh zonation. A shift in salt marsh zonation will likely be accompanied by alterations in greenhouse gas dynamics. This could be as extreme as switching from a net sink to a net source of $CH_4$, should an upland-transition area become regularly inundated. The potential link between salt marsh zonation and its $CO_2$ and $CH_4$ fluxes also points to the possibilities of better modeling the carbon dynamics of salt marsh ecosystems by incorporating information on their zonation, such as surface elevation, tidal frequency, and vegetation types and distribution. Tools that can provide valuable information on delineating salt marsh zonation, such as hyperspectral remote sensing and electromagnetic conductivity mapping, will therefore benefit future studies of wetland biogeochemistry.

## 5. References

Álvarez Rogel J, Ortiz Silla R, Alcaraz Ariza F (2001) Edaphic characterization and soil ionic composition influencing plant zonation in a semiarid Mediterranean salt marsh. Geoderma 99:81–98. doi: 10.1016/S0016-7061(00)00067-7

Bartlett KB, Bartlett DS, Harriss RC, Sebacher DI (1987) Methane emissions along a salt marsh salinity gradient. Biogeochemistry 4:183–202. doi: 10.1007/BF02187365

Bridgham SD, Cadillo-Quiroz H, Keller JK, Zhuang Q (2013) Methane emissions from wetlands: biogeochemical, microbial, and modeling perspectives from local to global scales. Glob Change Biol 19:1325–1346. doi: 10.1111/gcb.12131

Bridgham SD, Megonigal JP, Keller JK, et al. (2006) The carbon balance of North American wetlands. Wetlands 26:889–916.

Bu N-S, Qu J-F, Zhao H, et al. (2015) Effects of semi-lunar tidal cycling on soil $CO_2$ and $CH_4$ emissions: a case study in the Yangtze River estuary, China. Wetl Ecol Manag 23:727–736. doi: 10.1007/s11273-015-9415-5

Callaway JC, Borde AB, Diefenderfer HL, et al. (2012) Pacific Coast tidal wetlands. Wetl Habitats N Am Ecol Conserv Concerns p 103–116.

Callaway RM, Jones S, Ferren Jr. WR, Parikh A (1990) Ecology of a mediterranean-climate estuarine wetland at Carpinteria, California: plant distributions and soil salinity in the upper marsh. Can J Bot 68:1139–1146. doi: 10.1139/b90-144

Chanton JP, Martens CS, Kelley CA (1989) Gas transport from methane-saturated, tidal freshwater and wetland sediments. Limnol Oceanogr 34:807–819. doi: 10.4319/lo.1989.34.5.0807

Chen X, Slater L (2016) Methane emission through ebullition from an estuarine mudflat: 1.

A conceptual model to explain tidal forcing based on effective stress changes. Water Resour Res 52:4469–4485. doi: 10.1002/2015WR018058

Chmura GL, Anisfeld SC, Cahoon DR, Lynch JC (2003) Global carbon sequestration in tidal, saline wetland soils. Glob Biogeochem Cycles 17. doi: 10.1029/2002GB001917

Chmura GL, Kellman L, Guntenspergen GR (2011) The greenhouse gas flux and potential global warming feedbacks of a northern macrotidal and microtidal salt marsh. Environ Res Lett 6:044016. doi: 10.1088/1748-9326/6/4/044016

Christiansen JR, Levy-Booth D, Prescott CE, Grayston SJ (2016) Microbial and environmental controls of methane fluxes along a soil moisture gradient in a Pacific coastal temperate rainforest. Ecosystems 19:1255–1270. doi: 10.1007/s10021-016-0003-1

Ciais P, Sabine C, Bala G, et al. (2014) Carbon and other biogeochemical cycles. In: Climate change 2013: the physical science basis. Contribution of Working Group I to the Fifth Assessment Report of the Intergovernmental Panel on Climate Change. Cambridge University Press, pp 465–570. doi: 10.1017/CBO9781107415324.015.

Czepiel PM, Crill PM, Harriss RC (1995) Environmental factors influencing the variability of methane oxidation in temperate zone soils. J Geophys Res Atmospheres 100:9359–9364. doi: 10.1029/95JD00542

Deppe M, Knorr K-H, McKnight D, Blodau C (2010) Effects of short-term drying and irrigation on $CO_2$ and $CH_4$ production and emission from mesocosms of a northern bog and an alpine fen. Biogeochemistry 100:89–103. doi: 10.1007/s10533-010-9406-9

Dunfield P, Knowles R, Dumont R, Moore TR (1993) Methane production and consumption in temperate and subarctic peat soils: Response to temperature and pH. Soil Biol Biochem 25:321–326. doi: 10.1016/0038-0717(93)90130-4

Elgin, BK (2012) Soil Organic matter of natural and restored coastal wetland soils in southern California. Master's Thesis, UCLA: Environmental Health 0354. Retrieved from: http://escholarship.org/uc/item/4np1v5x3

Emery NC, Ewanchuk PJ, Bertness MD (2001) Competition and salt-marsh plant zonation: stress tolerators may be dominant competitors. Ecology 82:2471–2485.

Ferren, WR (1985) Carpinteria Salt Marsh: environment, history, and botanical resources of a southern California estuary. Herbarium, Dept. of Biological Sciences, University of California, Santa Barbara.

Fiedler S, Sommer M (2000) Methane emissions, groundwater levels and redox potentials of common wetland soils in a temperate-humid climate. Glob Biogeochem Cycles 14:1081–1093. doi: 10.1029/1999GB001255

Garcia J-L, Patel BK., Ollivier B (2000) Taxonomic, phylogenetic, and ecological diversity of methanogenic Archaea. Anaerobe 6:205–226. doi: 10.1006/anae.2000.0345

Gavlak R, Horneck D, Miller RO, Kotuby-Amacher J (2003) Soil, plant and water reference methods for the western region. WCC-103 Publ WREP-125 17–36.

Giani L, Dittrich K, Martsfeld-Hartmann A, Peters G (1996) Methanogenesis in saltmarsh soils of the North Sea coast of Germany. Eur J Soil Sci 47:175–182.

Gosselink JG, Hatton R, Hopkinson CS (1984) Relationship of organic carbon and mineral content to bulk density in Louisiana marsh soils. Soil Sci 137:177–180.

Itoh M, Kosugi Y, Takanashi S, et al. (2012) Effects of soil water status on the spatial variation of carbon dioxide, methane and nitrous oxide fluxes in tropical rain-forest soils in Peninsular Malaysia. J Trop Ecol 28:557–570. doi: 10.1017/S0266467412000569

Koh H-S, Ochs CA, Yu K (2009) Hydrologic gradient and vegetation controls on $CH_4$ and $CO_2$ fluxes in a spring-fed forested wetland. Hydrobiologia 630:271–286. doi: 10.1007/s10750-009-9821-x

Laanbroek HJ (2010) Methane emission from natural wetlands: interplay between emergent macrophytes and soil microbial processes. A mini-review. Ann Bot 105:141–153. doi: 10.1093/aob/mcp201

Le Mer J, Roger P (2001) Production, oxidation, emission and consumption of methane by soils: a review. Eur J Soil Biol 37:25–50.

Lessard R, Rochette P, Topp E, et al. (1994) Methane and carbon dioxide fluxes from poorly drained adjacent cultivated and forest sites. Can J Soil Sci 74:139–146. doi: 10.4141/cjss94-021

Magenheimer JF, Moore TR, Chmura GL, Daoust RJ (1996) Methane and carbon dioxide flux from a macrotidal salt marsh, Bay of Fundy, New Brunswick. Estuaries 19:139. doi: 10.2307/1352658

Martin RM, Moseman-Valtierra S (2015) Greenhouse gas fluxes vary between *Phragmites australis* and native vegetation zones in coastal wetlands along a salinity gradient. Wetlands 35:1021–1031. doi: 10.1007/s13157-015-0690-y

Masselink G, Hughes MG, Knight J (2011) Introduction to coastal processes & geomorphology. Hodder Education, London

Meijide A, Manca G, Goded I, et al. (2011) Seasonal trends and environmental controls of methane emissions in a rice paddy field in Northern Italy. Biogeosciences 8:3809–3821. doi: 10.5194/bg-8-3809-2011

Middelburg JJ, Klaver G, Nieuwenhuize J, et al. (1996) Organic matter mineralization in intertidal sediments along an estuarine gradient. Marine Ecology Progress Series: 157–168

Mitsch WJ, Bernal B, Nahlik AM, et al. (2013) Wetlands, carbon, and climate change. Landscape Ecology 28:583–597. doi: 10.1007/s10980-012-9758-8

Moffett KB, Robinson DA, Gorelick SM (2010) Relationship of salt marsh vegetation zonation to Spatial Patterns in Soil Moisture, Salinity, and Topography. Ecosystems 13:1287–1302. doi: 10.1007/s10021-010-9385-7

Moore T, De Young A, Bubier J, et al. (2011) A multi-year record of methane flux at the Mer Bleue Bog, southern Canada. Ecosystems 14:646–657. doi: 10.1007/s10021-011-9435-9

Moseman-Valtierra S, Abdul-Aziz OI, Tang J, et al. (2016) Carbon dioxide fluxes reflect plant zonation and belowground biomass in a coastal marsh. Ecosphere 7(11). doi: 10.1002/ecs2.1560

Nyman JA, DeLaune RD (1991) $CO_2$ emission and soil Eh responses to different hydrological conditions in fresh, brackish, and saline marsh soils. Limnol Oceanogr 36:1406–1414. doi: 10.4319/lo.1991.36.7.1406

Page HM, Petty RL, Meade DE (1995) Influence of watershed runoff on nutrient dynamics in a southern California salt marsh. Estuar Coast Shelf Sci 41:163–180.

Peinado M, Alcaraz F, Aguirre JL, et al. (1995) Similarity of zonation within Californian-Baja Californian and Mediterranean salt marshes. Southwest Nat 40:388–405.

Poffenbarger HJ, Needelman BA, Megonigal JP (2011) Salinity influence on methane emissions from tidal marshes. Wetlands 31:831–842. doi: 10.1007/s13157-011-0197-0

Sadro S, Gastil-Buhl M, Melack J (2007) Characterizing patterns of plant distribution in a southern California salt marsh using remotely sensed topographic and hyperspectral data and local tidal fluctuations. Remote Sens Environ 110:226–239. doi: 10.1016/j.rse.2007.02.024

Scavia D, Field JC, Boesch DF, et al. (2002) Climate change impacts on U.S. Coastal and Marine Ecosystems. Estuaries 25:149–164. doi: 10.1007/BF02691304

Silvestri S, Defina A, Marani M (2005) Tidal regime, salinity and salt marsh plant zonation. Estuar Coast Shelf Sci 62:119–130. doi: 10.1016/j.ecss.2004.08.010

Ström L, Mastepanov M, Christensen TR (2005) Species-specific effects of vascular plants on carbon turnover and methane emissions from wetlands. Biogeochemistry 75:65–82.

Sutton-Grier AE, Megonigal JP (2011) Plant species traits regulate methane production in freshwater wetland soils. Soil Biol Biochem 43:413–420. doi: 10.1016/j.soilbio.2010.11.009

Taillefert M, Neuhuber S, Bristow G (2007) The effect of tidal forcing on biogeochemical processes in intertidal salt marsh sediments. Geochem Trans 8:6. doi: 10.1186/1467-4866-8-6

Wachinger G, Fiedler S, Zepp K, et al. (2000) Variability of soil methane production on the micro-scale: spatial association with hot spots of organic material and Archaeal populations. Soil Biol Biochem 32:1121–1130. doi: 10.1016/S0038-0717(00)00024-

9

Wang C, Tong C, Chambers LG, Liu X (2017) Identifying the salinity thresholds that impact greenhouse gas production in subtropical tidal freshwater marsh soils. Wetlands 37:559–571. doi: 10.1007/s13157-017-0890-8

Wilson BJ, Mortazavi B, Kiene RP (2015) Spatial and temporal variability in carbon dioxide and methane exchange at three coastal marshes along a salinity gradient in a northern Gulf of Mexico estuary. Biogeochemistry 123:329–347. doi: 10.1007/s10533-015-0085-4

Xu X, Zou X, Cao L, et al. (2014) Seasonal and spatial dynamics of greenhouse gas emissions under various vegetation covers in a coastal saline wetland in southeast China. Ecol Eng 73:469–477. doi: 10.1016/j.ecoleng.2014.09.087

Yuan J, Ding W, Liu D, et al. (2014) Methane production potential and methanogenic archaea community dynamics along the *Spartina alterniflora* invasion chronosequence in a coastal salt marsh. Appl Microbiol Biotechnol 98:1817–1829. doi: 10.1007/s00253-013-5104-6

Yu J, Lv X, Bin M, et al. (2015) Fractal features of soil particle size distribution in newly formed wetlands in the Yellow River Delta. Sci Rep 5: srep10540. doi: 10.1038/srep10540